Abstract

Measurement of total hadronic differential cross sections in the LArIAT experiment

Elena Gramellini

2018

Abstract goes here. Limit 750 words.

Measurement of total hadronic differential cross sections in the LArIAT experiment

A Dissertation
Presented to the Faculty of the Graduate School
of
Yale University
in Candidacy for the Degree of
Doctor of Philosophy

by
Elena Gramellini

Dissertation Director: Bonnie T. Fleming

Date you'll receive your degree

Contents

Acknowledgements **iv**

0 Hadron Interactions in Argon: Cross Section **1**

0.1 How to Measure a Hadron Cross Section in LArIAT 1

0.1.1 Event Selection 2

0.1.2 Wire Chamber to TPC Match 4

0.1.3 The Thin Slice Method 5

0.1.4 Procedure testing with truth quantities 8

1 Samples Preparation **11**

1.1 LArIAT Data 11

1.2 LArIAT Monte Carlo 11

1.2.1 G4Beamline 11

1.2.2 Data Driven MC 11

1.3 Energy Calibration 11

1.4 Tracking Studies 11

1.4.1 Selection Study for the Wire Chamber to TPC Match 12

1.4.2 Interaction Point Optimization 15

1.4.3 Tracking spatial and angular resolution 16

1.4.4 Estimate of E_{loss} before the TPC 16

Acknowledgements

A lot of people are awesome, especially you, since you probably agreed to read this when it was a draft.

Chapter 0

Hadron Interactions in Argon: Cross Section

0.1 How to Measure a Hadron Cross Section in LArIAT

We use both the LArIAT beamline detectors and the LArTPC information to measure hadronic cross sections in argon. Albeit with small differences, both the π^- - Ar and K^+ - Ar total hadronic cross section measurements rely on the same procedure described in details in the following paragraphs: we select the particle of interest using a combination of beamline detectors and TPC information (paragraph 0.1.1), we perform a handshake between the beamline information and the TPC tracking to assure we are selecting the right TPC track (paragraph 0.1.2), and we apply the "thin slice" method to get to the final result (paragraph 0.1.3). We show a cross check of this method in paragraph 0.1.4.

0.1.1 Event Selection

Beamline events

As will be clear in paragraph 0.1.3, beamline particle identification and momentum measurement before entering the TPC are fundamental information for the hadronic cross sections measurements in LArIAT. Thus, we scan the LArIAT data to keep only events whose wire chamber and time of flight information is registered. Additionally, we perform a check of the plausibility of the trajectory inside the beamline detectors: given the position of the hits in the four wire chambers, we make sure the particle trajectory does not cross any impenetrable material such as the collimator and the magnets steel.

Particle Identification in the beamline

In data, the main tool to establish the identity of the hadron of interest is the LArIAT tertiary beamline, in its function of mass spectrometer. We combine the measurement of the time of flight, TOF, and the beamline momentum, p_{Beam}, to reconstruct the invariant mass of the particles in the beamline, m_{Beam}, as follows

$$m_{Beam} = \frac{p_{Beam}}{c}\sqrt{\left(\frac{TOF * c}{l}\right)^2 - 1}, \tag{1}$$

where c is the speed of light and l is the length of the particle trajectory between the time of flight paddels.

Figure 1 shows the mass distribution for the Run II negative polarity runs on the left and positive polarity runs on the right. We perform the classification of events into the different samples as follows:

- $\underline{\pi, \mu, e}$: 0 MeV < mass < 350 MeV
- <u>kaon:</u> 350 MeV < mass < 650 MeV

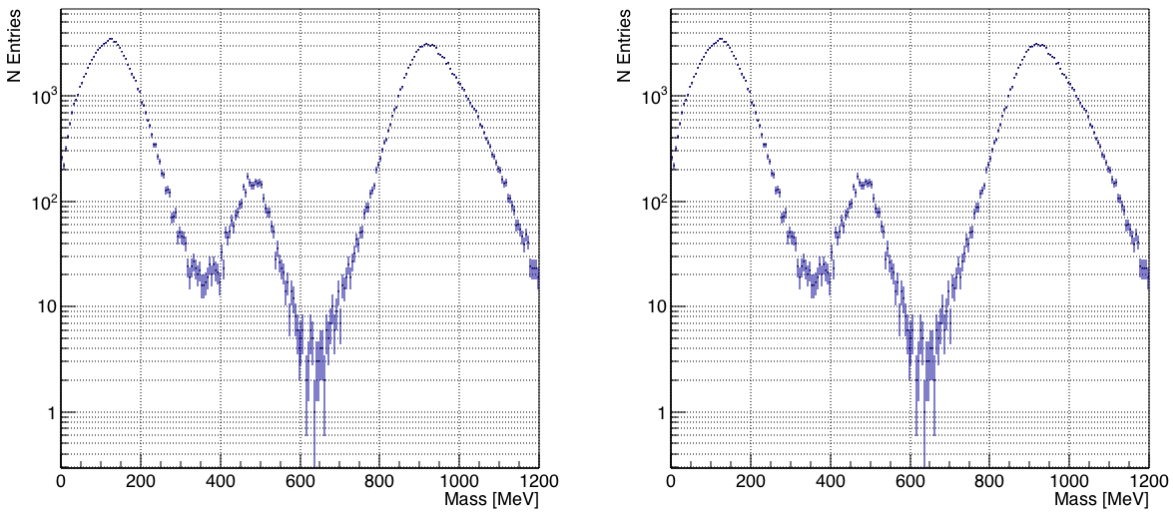

Figure 1: The mass plotted for a sample of Run-II events reconstructed in the beamline, negative polarity runs on the left and positive polarity runs on the right. The classification of the events into π, μ, e, kaon, or proton is based on this distribution.CHANGE PLOTS

- proton: 650 MeV $<$ mass $<$ 3000 MeV.

Additional Particle Identification technique

In the case of the π^--Ar cross section, the resolution of beamline mass spectrometer is not sufficient to select a beam of pure pions. In fact, muons and electrons survive the selection on the beamline mass value. It is important to notice that the composition of the negative polarity beam is mostly pions, as discussed in **??**. Anyhow, we devise a selection on the TPC information to mitigate the presence of electrons in the sample used for the pion cross section. The selection relies on the different topologies of a pion and an electron event in the argon: while the former will trace a track inside the TPC active volume, the latter will tend to "shower", i.e. interact with the medium, produce bremsstrahlung photons which pair convert into several short tracks. We provide details of this selection in section **??**.

Pile up mitigation

The secondary beam impinging on LArIAT secondary target produces a plethora of particles. The presence of upstream and downstream collimators greatly abates the number of particles tracing down the LArIAT beamline. However, more than one beamline particles, or particles produced from the beam interaction with the beamline detectors, may sneak into the LArTPC during its readout time. The TPC readout is triggered by the actual particle firing the beamline detectors; we call "pile up" the additional traces in the TPC. We adjusted the primary beam intensity between LArIAT Run I and Run II to minimize the presence of events with high pile up particles in the data sample. For the cross section analyses, we remove events with more than 4 tracks in the first 14 cm upstream portion of the TPC from the sample. probably need to do a better job explaining pile up

0.1.2 Wire Chamber to TPC Match

For each event passing the selection on its beamline information we need to identify the track inside the TPC corresponding to the particle which triggered the beamline detectors, a procedure we refer to as "WC to TPC match" (WC2TPC for short). In general, the TPC tracking algorithm will reconstruct more than one track in the event, partially due to the fact that hadrons interact in the chamber, as shown in figure **??**, and partially because of pile up particles during the triggered TPC drift time, as shown in figure **??**. ADD EVENT DISPLAYS

We attempt to uniquely match one wire chamber track to one and only one reconstructed TPC track. In data, this match leverages on a geometrical selection exploiting both the position of the wire chamber and TPC tracks, and the angle between them. We consider only TPC tracks whose first point is in the first 2 cm upstream portion of the TPC for the match. We project the wire chamber track to the TPC front face where we define the x_{FF} and y_{FF} coordinates used for evaluating the

match. We define ΔX as the difference between the x position of the most upstream point of the TPC track and x_{FF}. ΔY is defined analogously. We define the radius difference, ΔR, as $\Delta R = \sqrt{\Delta X^2 + \Delta Y^2}$. The angle between the incident WC track and the TPC track in the plane that contains them defines α. If $\Delta R < 4$ cm, $\alpha < 8°$, a match between WC-track and TPC reconstructed track is found. We describe how we determinate the best value for the radius and angular selection in sec 1.4.1. In MC, we mimic the matching between the WC and the TPC track by constructing a fake WC track using truth information at wire chamber four. We then apply the same WC to TPC matching algorithm as in data. We discard events with multiple WC2TPC matches. We use only TPC track matched to WC tracks in the cross section calculation.

0.1.3 The Thin Slice Method

Cross Sections on Thin Target

Cross section measurements on a thin target have been the bread and butter of nuclear and particle experimentalists since the Rutherford experiments NEED CITATION. At their core, this type of experiments consists in shooting a beam of particles with a known flux on a thin target and recording the outgoing flux.

In general, the target is not a single particle, but rather a slab of material containing many diffusion centers. The so-called "thin target" approximation assumes that the target centers are uniformly distributed in the material and that the target is thin compared to the interaction length so that no center of interaction sits in front of another. In this approximation, the ratio between the number of particles interacting in the target $N_{Interacting}$ and number of incident particles $N_{Incident}$ determines the interaction probability $P_{Interacting}$, which is the complementary to one of the survival

probability $P_{Survival}$. Equation 2

$$P_{Survival} = 1 - P_{Interacting} = 1 - \frac{N_{Interacting}}{N_{Incident}} = e^{-\sigma_{TOT} n \delta X} \tag{2}$$

describes the probability for a particle to survive the thin target. This formula relates the total cross section σ_{TOT}, the density of the target centers n and the thickness of the target along the incident hadron direction δX, to the interaction probability[1]. If the target is thin compared to the interaction length of the process considered, we can Taylor expand the exponential function in equation 2 and find a simple proportionality relationship between the number of incident and interacting particles, and the cross section, as shown in equation 3:

$$1 - \frac{N_{Interacting}}{N_{Incident}} = 1 - \sigma_{TOT} n \delta X + O(\delta X^2). \tag{3}$$

Solving for the cross section, we find:

$$\sigma_{TOT} = \frac{1}{n \delta X} \frac{N_{Interacting}}{N_{Incident}}. \tag{4}$$

Not-so-Thin Target: Slicing the Argon

The LArIAT TPC, with its 90 cm of length, is not a thin target. Find expected interaction length for hadrons and kaons. However, the fine-grained tracking of the LArIAT LArTPC allows us to treat the argon volume as a sequence of many adjacent thin targets.

As described in section **??**, LArIAT wire planes count 240 wires each. The wires are oriented at +/- 60° from the vertical direction at 4 mm spacing, while the beam direction is oriented 3 degrees off the z axis in the XZ plane. review this math The

1. The scattering center density in the target, n, relates to the argon density ρ, the Avogadro number N_A and the argon molar mass m_A as $n = \frac{\rho N_A}{m_A}$.

wires collect signals proportional to the energy loss of the hadron along its path in a $\delta X = 4$ mm/sin(60°) ≈ 4.7 mm slab of liquid argon. Thus, one can think to slice the TPC into many thin targets of $\delta X = 4.7$ mm thickness along the direction of the incident particle.

Considering each slice j a "thin target", we can apply the cross section calculation from Eq. 4 iteratively, evaluating the kinetic energy of the hadron as it enters each slice, E_j^{kin}. For each WC-to-TPC matched particle, the energy of the hadron entering the TPC is known thanks to the momentum and mass determination by the tertiary beamline,

$$E_{FrontFace}^{kin} = \sqrt{p_{Beam}^2 - m_{Beam}^2} - m_{Beam} - E_{loss}, \tag{5}$$

where E_{loss} is a correction for the energy loss in the dead material between the beamline and the TPC front face (more on **??**). The energy of the hadron at the each slab is determined by subtracting the energy released by the particle in the previous slabs. For example, at the j^{th} point of a track, the kinetic energy will be

$$E_j^{kin} = E_{FrontFace}^{kin} - \sum_{i<j} \Delta E_i, \tag{6}$$

where ΔE_i is the energy deposited at each argon slice before the j^{th} point as measured by the calorimetry associated with the tracking.

If the particle enters a slice, it contributes to $N_{Incident}(E^{kin})$ in the energy bin corresponding to its kinetic energy in that slice. If it interacts in the slice, it then also contributes to $N_{Interacting}(E^{kin})$ in the appropriate energy bin. The cross section as a function of kinetic energy, $\sigma_{TOT}(E^{kin})$ will then be proportional to the ratio $\frac{N_{Interacting}(E^{kin})}{N_{Incident}(E^{kin})}$.

The statistical uncertainty for each energy bin is calculated by error propagation from the statistical uncertainty on $N_{Incident}$ and $N_{Interacting}$. Since the number of

incident hadrons in each energy bin is given by a simple counting, we assume that $N_{Incident}$ is distributed as a poissonian with mean and σ^2 equal to $N_{Incident}$ in each bin. On the other hand, $N_{Interacting}$ follows a binomial distribution: a particle in a given energy bin might or might not interact. The square of the variance for the binomial is given by

$$\sigma^2 = \mathcal{N} P_{Interacting}(1 - P_{Interacting}); \tag{7}$$

since the interaction probability $P_{Interacting}$ is $\frac{N_{Interacting}}{N_{Incident}}$ and the number of tries $\mathcal{N}$ is $N_{Incident}$, equation 7 translates into

$$\sigma^2 = N_{Incident}\frac{N_{Interacting}}{N_{Incident}}(1 - \frac{N_{Interacting}}{N_{Incident}}) = N_{Interacting}(1 - \frac{N_{Interacting}}{N_{Incident}}). \tag{8}$$

$N_{Incident}$ and $N_{Interacting}$ are not independent. The uncertainty on the cross section is thus calculated as

$$\delta\sigma_{tot}(E) = \sigma_{tot}(E)\Big(\frac{\delta N_{Interacting}}{N_{Interacting}} + \frac{\delta N_{Incident}}{N_{Incident}}\Big) \tag{9}$$

where:

$$\delta N_{Incident} = \sqrt{N_{Incident}} \tag{10}$$

$$\delta N_{Interacting} = \sqrt{N_{Interacting}\Big(1 - \frac{N_{Interacting}}{N_{Incident}}\Big)}. \tag{11}$$

0.1.4 Procedure testing with truth quantities

The π^--Ar and K^+-Ar total hadronic cross section implemented in Geant4 can be used as a tool to validate the measurement methodology. We describe here a closure test done on Monte Carlo to prove that the methodology of slicing the TPC retrieves the underlying cross section distribution implemented in Geant4 within the statistical error.

For pions in the considered energy range, the Geant4 inelastic model adopted to is "BertiniCascade", while the elastic model "hElasticLHEP". For kaons, the Geant4 inelastic model adopted to is "BertiniCascade", while the elastic model "hElasticLHEP".

For the validation test, we fire about 390000 pions and 140000 kaons inside the LArIAT TPC active volume using the DDMC (see sec **??**). We apply the thin-sliced method on using true quantities to calculate the hadron kinetic energy at each slab in order to decouple reconstruction effects to eventual issues with the methodology. For each slab of 4.7 mm length on the path of the hadron, we integrate the true energy deposition as given by the Geant4 transportation model. Then, we recursively subtracted it from the hadron kinetic energy at the TPC front face to evaluate the kinetic energy at each slab until the true interaction point is reached. Doing so, we obtain the true interacting and incident distributions for the considered hadron and we obtain the true MC cross section as a function of the hadron true kinetic energy.

Figure **??** shows the total hadronic cross section for argon implemented in Geant4 10.01.p3 (solid lines) overlaid with the true MC cross section as obtained with the sliced TPC method (markers) for pions on the left and kaons on the right; the total cross section is shown in green, the elastic cross section in blue and the inelastic cross section in red. The nice agreement with the Geant4 distribution and the cross section obtained with the sliced TPC method gives us confidence in the validity of the methodology.

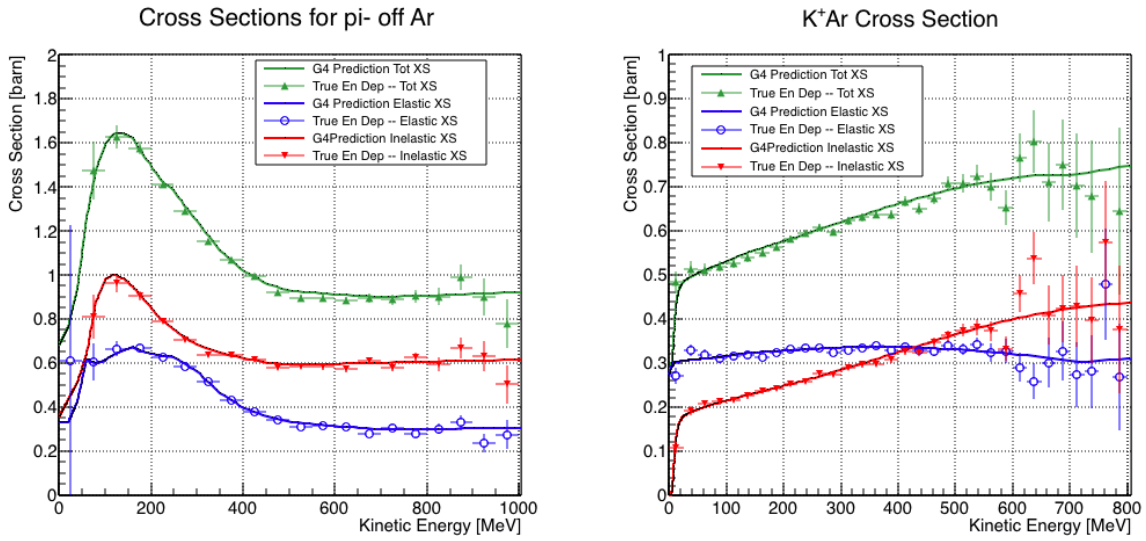

Figure 2: Hadronic cross sections for π^--Ar (left) and K^+-Ar (right) implemented in Geant4 10.01.p3 (solid lines) overlaid the true MC cross section as obtained with the sliced TPC method (markers). The total cross section is shown in green, the elastic cross section in blue and the inelastic cross section in red.

Chapter 1

Samples Preparation

This chapter describes the data and Monte Carlo samples used for the cross section analyses,

1.1 LArIAT Data

1.2 LArIAT Monte Carlo

1.2.1 G4Beamline

1.2.2 Data Driven MC

1.3 Energy Calibration

1.4 Tracking Studies

In this section, we describe three studies. The first is a justification of the selection criteria for the beamline handshake with the TPC information. We perform this study to boost the correct identification of the particles in the TPC associated with

the beamline information, while maintaining sufficient statistics for the cross section measurement. The second study is an optimization of the tracking algorithm, with the scope of maximizing the identification of the hadronic interaction point inside the TPC. These two studies are related, since the optimization of the tracking is performed on TPC tracks which have been matched to the wire chamber track; in turn, the tracking algorithm for TPC tracks determine the number of reconstructed tracks in each event used to try the matching with the wire chamber track. Starting with a sensible tracking reconstruction, we perform the WC2TPC matching optimization first, then the tracking optimization. The WC2TPC match purity and efficiency are then calculated again with the optimized tracking.

We perform the following studies on a MC sample of 191000 kaons and 359000 pions produced with the DDMC technique. DDMC particles are shot from the WC4 location into the TPC following the beam profile. We mimic the matching between the WC and the TPC track on Monte Carlo by constructing a fake WC track using truth information at wire chamber four. We then apply the same WC to TPC matching algorithm as in data described in 0.1.2.

1.4.1 Selection Study for the Wire Chamber to TPC Match

Plots I want in this section:

1. WC2TPC MC DeltaX, DeltaY and α

Scope of this study is assessing the goodness of the wire chamber to TPC match on Monte Carlo and decide the selection values we will use on data. A word of caution is necessary here. With this study, we want to minimize pathologies associated with the presence of the primary hadron itself, e.g. the incorrect association between the beamline hadron and its decay products inside the TPC. Assessing the contamination from pile-up[1], albeit related, is beyond the scope of this study.

1. We remind the reader that the DDMC is a single particle Monte Carlo, where the beam pile

In MC, we are able to define a correct WC2TPC match using the Geant4 truth information. We are thus able to count how many times the WC tracks is associated with the wrong TPC reconstructed track.

We define a correct match if the all following conditions are met:

- the length of the true primary Geant4 track in the TPC is greater than 2 cm,
- the length of the reconstructed track length is greater than 2 cm,
- the Z position of the first reconstructed point is within 2 cm from the TPC front face
- the distance between the reconstructed track and the true entering point is the minimum compared with all the other reconstructed tracks.

In order to count the wrong matches, we consider all the reconstructed tracks whose Z position of the first reconstructed point lies within 2 cm from the TPC front face. Events with true length in TPC < 2 cm are included. Since hadrons are shot 100 cm upstream from the TPC front face, the following two scenarios are possible from a truth standpoint:

[Ta] the primary hadron decays or interact strongly before getting to the TPC,

[Tb] the primary hadron enters the TPC.

Once we choose the selection cuts to determine a reconstructed wire chamber-to-TPC match r_T and α_T, the following five scenarios are possible in the truth to reconstruction interplay :

1) only the correct track is matched

2) only one wrong track is matched

up is not simulated.

3) the correct track and one (or more) wrong tracks are matched

4) multiple wrong tracks matched.

5) no reconstructed tracks are matched

Since we keep only events with one and only one match, we discard cases 3), 4) and 5) from the events used in the cross section measurement. For each set of r_T and α_T selection value, we define purity and efficiency of the selection as follows:

$$\text{Efficiency} = \frac{\text{Number of events correctly matched}}{\text{Number of events with primary in TPC}} \tag{1.1}$$

$$\text{Purity} = \frac{\text{Number of events correctly matched}}{\text{Total number of matched events}}. \tag{1.2}$$

Figure 1.1 shows the efficiency (left) and purity (right) for wire chamber-to-TPC match as a function of the radius, r_T, and angle, α_T, selection value. It is apparent how both efficiency and purity are fairly flat as a function of the radius selection value at a given angle. This is not surprising. Since we are studying a single particle gun Monte Carlo sample, the wrong matches can occur only for mis-tracking of the primary or for association with decay products; decay products will tend to be produced at large angles compared to the primary, but could be fairly close to the in x and y projection of the primary. The radius cut would play a key role in removing pile up events.

For LArIAT cross section measurements, we generally prefer purity over efficiency, since a sample of particles of a pure species will lead to a better measurement. Obviously, purity should be balanced with a sensible efficiency to avoid rejecting the whole sample.

We choose (α_T, r_T) = (8 deg, 4 cm) and get a MC 85% efficiency and 98% purity for the kaon sample and a MC BOH% efficiency and 98% purity for the BOH sample.

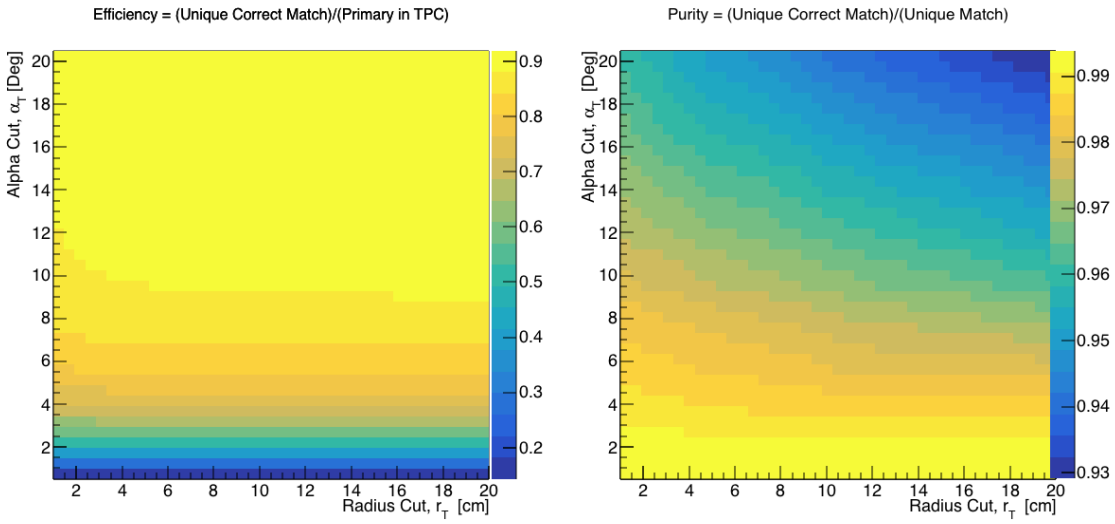

Figure 1.1: Efficiency (left) and purity (right) for wire chamber-to-TPC match as a function of the radius and angle selections.

1.4.2 Interaction Point Optimization

Scheme of this subsection

Brief Explanation of the reconstruction chain

Explanation of clustering parameters

Figure of merit and spanning of cluster

Important numbers out of this optimization

Plots I want in this section:

1. Delta L, reco - true
2. Delta L, reco - true Elastic, Delta L, reco - true Inelastic, other
3. Length Quality cut
4. Efficiency as a function of true KE and Angle

1.4.3 Tracking spatial and angular resolution

Scope of this study is understanding and comparing the tracking spatial and angular resolution on data and MC. We start by selecting all the WC2TPC matched tracks. We fit a line on all the space points of the track and calculate the χ^2. The χ^2 distribution for data and MC is shown in Figure **??**.

For the spatial and angular resolution study, we reject tracks with less than 14 space points. For each track, we order the space points according to their Z position and we split them in two sets: the first set counts all the points belonging to the first half of the track and the second set counts all the points belonging to the second half of the track. We remove the last 5 points in the first set and the first 5 points in the second set, so to have a gap in the middle of the original track. We fit the first and the second set of points with a line separately. We reject the event entirely if the χ^2 for the fit of either of the halves is greater than four. We define a track middle plane as the plane perpendicular to the original track fit, positioned in the middle of its length. We project the tracks on the middle plane and calculate the impact parameter, d, i.e. the distance between the projected points. We also calculate the angle between the original track direction and the fit of the first and second half, called α_1 and α_2 respectively. The spatial resolution of the track will be $\sigma_S = \frac{d}{\sqrt{2}}$ while the angular resolution of the tracks will be $\sigma_\alpha = \alpha_1 - \alpha_2$. The distributions for data and MC for σ_α and σ_S are given in **??**.

1.4.4 Estimate of E_{loss} before the TPC

The beamline particles travel a path from when their momentum is measured by the beamline detector, until they are tracked inside the TPC. In the current LArIAT geometry, a particle leaving the fourth wire chamber will encounter the materials listed in Table 1.1 before being registered again. The energy lost by the particle in this non instrumented material modifies the particle's kinetic energy and directly

affects the cross section measurement, as shown in equation 5.

Material	density [g/cm^3]	width [cm]
Fiberglass laminate (G10)	1.7	1.28
Liquid Argon	1.4	3.72
Stainless Steel	7.7	0.23
Titanium	4.5	0.04
Air	$1.2 \cdot 10^{-3}$	89.43
Plastic Scintillator	1.03	5.30

Table 1.1: LArIAT material budget from WC4 to the TPC Front Face.

We estimate the uncertainty on the energy loss between the beamline momentum measurement and the TPC, E_{loss}, using the DDMC pion sample. We shoot pions from WC4 with the same momentum distribution as in the beamline data and plot the true E_{loss} for that sample. The distribution for E_{loss} for the pion sample is shown in Figure 1.2. We estimate the energy loss for pions to be $E_{loss} = 37 \pm 7$ MeV where we use the average energy lost as the central value and the standard deviation of the distribution as the uncertainty.

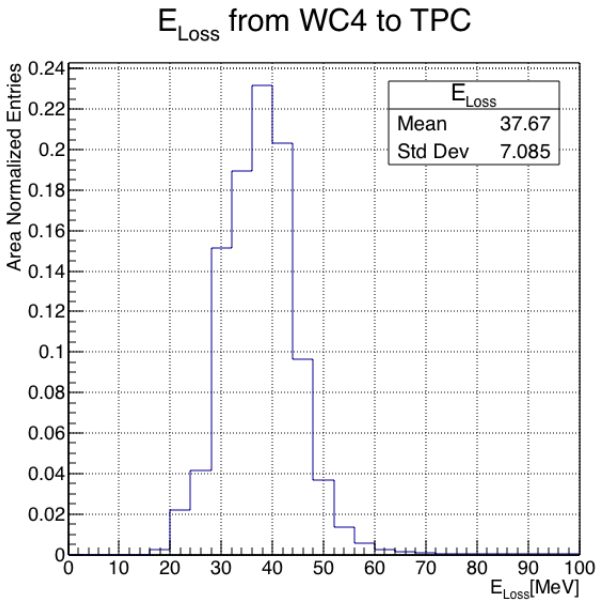

Figure 1.2: Energy loss by simulated negative pions downstream from WC4 and upstream from the TPC.

Bibliography

[1] Precision electroweak measurements on the z resonance. *Physics Reports*, 427(5):257 – 454, 2006.

[2] R. Acciarri et al. Demonstration and Comparison of Operation of Photomultiplier Tubes at Liquid Argon Temperature. *JINST*, 7:P01016, 2012.

[3] A. Aguilar-Arevalo et al. Evidence for neutrino oscillations from the observation of anti-neutrino(electron) appearance in a anti-neutrino(muon) beam. *Phys. Rev.*, D64:112007, 2001.

[4] A. A. Aguilar-Arevalo et al. Improved Search for $\bar{\nu}_\mu \to \bar{\nu}_e$ Oscillations in the MiniBooNE Experiment. *Phys. Rev. Lett.*, 110:161801, 2013.

[5] C. Anderson et al. The ArgoNeuT Detector in the NuMI Low-Energy beam line at Fermilab. *JINST*, 7:P10019, 2012.

[6] C. Andreopoulos et al. The GENIE Neutrino Monte Carlo Generator. *Nucl. Instrum. Meth.*, A614:87–104, 2010.

[7] D. Ashery, I. Navon, G. Azuelos, H. K. Walter, H. J. Pfeiffer, and F. W. Schlepütz. True absorption and scattering of pions on nuclei. *Phys. Rev. C*, 23:2173–2185, May 1981.

[8] C. Athanassopoulos et al. Evidence for nu(mu) $\to$ nu(e) neutrino oscillations from LSND. *Phys. Rev. Lett.*, 81:1774–1777, 1998.

[9] Borut Bajc, Junji Hisano, Takumi Kuwahara, and Yuji Omura. Threshold corrections to dimension-six proton decay operators in non-minimal {SUSY} su(5) {GUTs}. *Nuclear Physics B*, 910:1 – 22, 2016.

[10] BASF Corp. 100 Park Avenue, Florham Park, NJ 07932 USA.

[11] A. Bodek and J. L. Ritchie. Further studies of fermi-motion effects in lepton scattering from nuclear targets. *Phys. Rev. D*, 24:1400–1402, Sep 1981.

[12] D. V. Bugg, R. S. Gilmore, K. M. Knight, D. C. Salter, G. H. Stafford, E. J. N. Wilson, J. D. Davies, J. D. Dowell, P. M. Hattersley, R. J. Homer, A. W. O'dell, A. A. Carter, R. J. Tapper, and K. F. Riley. Kaon-nucleon total cross sections from 0.6 to 2.65 gev/ *c*. *Phys. Rev.*, 168:1466–1475, Apr 1968.

[13] A. S. Carroll, I. H. Chiang, C. B. Dover, T. F. Kycia, K. K. Li, P. O. Mazur, D. N. Michael, P. M. Mockett, D. C. Rahm, and R. Rubinstein. Pion-nucleus total cross sections in the (3,3) resonance region. *Phys. Rev. C*, 14:635–638, Aug 1976.

[14] D. Casper. The nuance neutrino physics simulation, and the future. *Nuclear Physics B - Proceedings Supplements*, 112(1-3):161–170, nov 2002.

[15] A. Cervera, A. Donini, M.B. Gavela, J.J. Gomez Cádenas, P. Hernández, O. Mena, and S. Rigolin. Golden measurements at a neutrino factory. *Nuclear Physics B*, 579(1-2):17–55, jul 2000.

[16] ATLAS Collaboration. Observation of a new particle in the search for the standard model higgs boson with the ATLAS detector at the LHC. *Physics Letters B*, 716(1):1–29, sep 2012.

[17] CMS Collaboration. Observation of a new boson at a mass of 125 gev with the cms experiment at the lhc. *Physics Letters B*, 716(1):30 – 61, 2012.

[18] Savas Dimopoulos, Stuart Raby, and Frank Wilczek. Proton Decay in Supersymmetric Models. *Phys. Lett.*, B112:133, 1982.

[19] D. Drakoulakos et al. Proposal to perform a high-statistics neutrino scattering experiment using a fine-grained detector in the NuMI beam. 2004.

[20] Torleif Ericson and Wolfram Weise. *Pions and Nuclei (The International Series of Monographs on Physics)*. Oxford University Press, 1988.

[21] A.A. Aguilar-Arevalo et al. The miniboone detector. *Nuclear Instruments and Methods in Physics Research Section A: Accelerators, Spectrometers, Detectors and Associated Equipment*, 599(1):28 – 46, 2009.

[22] Antonio Bueno et al. Nucleon decay searches with large liquid argon TPC detectors at shallow depths: atmospheric neutrinos and cosmogenic backgrounds. *Journal of High Energy Physics*, 2007(04):041–041, apr 2007.

[23] A.S. Clough et al. Pion-nucleus total cross sections from 88 to 860 MeV. *Nuclear Physics B*, 76(1):15–28, jul 1974.

[24] B.W. Allardyce et al. Pion reaction cross sections and nuclear sizes. *Nuclear Physics A*, 209(1):1 – 51, 1973.

[25] C Athanassopoulos et al. The liquid scintillator neutrino detector and LAMPF neutrino source. *Nuclear Instruments and Methods in Physics Research Section A: Accelerators, Spectrometers, Detectors and Associated Equipment*, 388(1-2):149–172, mar 1997.

[26] F. Binon et al. Scattering of negative pions on carbon. *Nuclear Physics B*, 17(1):168 – 188, 1970.

[27] L. Aliaga et al. Minerva neutrino detector response measured with test beam data. *Nuclear Instruments and Methods in Physics Research Section A: Accelerators, Spectrometers, Detectors and Associated Equipment*, 789:28 – 42, 2015.

[28] M Adamowski et al. The liquid argon purity demonstrator. *Journal of Instrumentation*, 9(07):P07005, 2014.

[29] P. Vilain et al. Coherent single charged pion production by neutrinos. *Physics Letters B*, 313(1-2):267–275, aug 1993.

[30] H Fenker. Standard beam pwc for fermilab. Technical report, Fermi National Accelerator Lab., Batavia, IL (USA), 1983.

[31] H Fesbach. Theoretical nuclear physics: Nuclear reactions. 1992.

[32] J. A. Formaggio and G. P. Zeller. From ev to eev: Neutrino cross sections across energy scales. *Rev. Mod. Phys.*, 84:1307–1341, Sep 2012.

[33] E. Friedman et al. K+ nucleus reaction and total cross-sections: New analysis of transmission experiments. *Phys. Rev.*, C55:1304–1311, 1997.

[34] Howard Georgi and S. L. Glashow. Unity of all elementary-particle forces. *Phys. Rev. Lett.*, 32:438–441, Feb 1974.

[35] D.Y. Wong (editor) G.L. Shaw (Editor). *Pion-nucleon Scattering*. John Wiley & Sons Inc, 1969.

[36] Glassman High Voltage, Inc., Precision Regulated High Voltage DC Power Supply.

[37] D S Gorbunov. Sterile neutrinos and their role in particle physics and cosmology. *Physics-Uspekhi*, 57(5):503, 2014.

[38] S. Hansen, D. Jensen, G. Savage, E. Skup, and A. Soha. Fermilab test beam multi-wire proportional chamber tracking system upgrade. June 2014. International Conference on Technology and Instrumentation in Particle Physics (TIPP 2014).

[39] Peter W. Higgs. Broken symmetries and the masses of gauge bosons. *Physical Review Letters*, 13(16):508–509, oct 1964.

[40] P.W. Higgs. Broken symmetries, massless particles and gauge fields. *Physics Letters*, 12(2):132–133, sep 1964.

[41] C. Jarlskog. A basis independent formulation of the connection between quark mass matrices, CP violation and experiment. *Zeitschrift für Physik C Particles and Fields*, 29(3):491–497, sep 1985.

[42] Cezary Juszczak, Jarosław A. Nowak, and Jan T. Sobczyk. Simulations from a new neutrino event generator. *Nuclear Physics B - Proceedings Supplements*, 159:211–216, sep 2006.

[43] D. I. Kazakov. Beyond the standard model: In search of supersymmetry. In *2000 European School of high-energy physics, Caramulo, Portugal, 20 Aug-2 Sep 2000: Proceedings*, pages 125–199, 2000.

[44] Dae-Gyu Lee, R. N. Mohapatra, M. K. Parida, and Merostar Rani. Predictions for the proton lifetime in minimal nonsupersymmetric so(10) models: An update. *Phys. Rev. D*, 51:229–235, Jan 1995.

[45] Ettore Majorana. Teoria simmetrica dell'elettrone e del positrone. *Il Nuovo Cimento*, 14(4):171–184, apr 1937.

[46] FM Newcomer, S Tedja, R Van Berg, J Van der Spiegel, and HH Williams. A fast, low power, amplifier-shaper-discriminator for high rate straw tracking systems. *IEEE Transactions on Nuclear Science*, 40(4):630–636, 1993.

[47] Emmy Noether. Invariant variation problems. *Transport Theory and Statistical Physics*, 1(3):186–207, jan 1971.

[48] S. Pascoli, S.T. Petcov, and A. Riotto. Leptogenesis and low energy cp-violation in neutrino physics. *Nuclear Physics B*, 774(1):1 – 52, 2007.

[49] C. Patrignani et al. Review of Particle Physics. *Chin. Phys.*, C40(10):100001, 2016.

[50] B. Pontecorvo. Neutrino Experiments and the Problem of Conservation of Leptonic Charge. *Sov. Phys. JETP*, 26:984–988, 1968. [Zh. Eksp. Teor. Fiz.53,1717(1967)].

[51] Steve Ritz et al. Building for Discovery: Strategic Plan for U.S. Particle Physics in the Global Context. 2014.

[52] L.M. Saunders. Electromagnetic production of pions from nuclei. *Nucl. Phys., B7: 293-310(1968).*

[53] Sigma-Aldrich, P.O. Box 14508, St. Louis, MO 63178 USA.

[54] D.R.O. Morrison N. Rivoire V. Flaminio, W.G. Moorhead. Compilation of Cross Sections I: π^+ and π^- Induced Reactions. *CERN-HERA*, pages 83–01, 1983.

[55] D.R.O. Morrison N. Rivoire V. Flaminio, W.G. Moorhead. Compilation of Cross Sections II: K^+ and K^- Induced Reactions. *CERN-HERA*, pages 83–02, 1983.

[56] Hermann Weyl. Gravitation and the electron. *Proceedings of the National Academy of Sciences of the United States of America*, 15(4):323–334, 1929.

[57] Colin et al Wilkin. A comparison of pi+ and pi- total cross-sections of light nuclei near the 3-3 resonance. *Nucl. Phys.*, B62:61–85, 1973.

[58] D. H. Wright and M. H. Kelsey. The Geant4 Bertini Cascade. *Nucl. Instrum. Meth.*, A804:175–188, 2015.

[59] C. S. Wu, E. Ambler, R. W. Hayward, D. D. Hoppes, and R. P. Hudson. Experimental test of parity conservation in beta decay. *Phys. Rev.*, 105:1413–1415, Feb 1957.

[60] T. Yanagida. Horizontal symmetry and masses of neutrinos. *Progress of Theoretical Physics*, 64(3):1103–1105, sep 1980.